### RECOMMENDATIONS FOR THE SHAPE OF THE DESIGN RESPONSE SPECTRUM IN THE NEW ZEALAND SEISMIC LOADINGS TECHNICAL SPECIFICATION

# Tom C. Francis<sup>1</sup>, Timothy J. Sullivan<sup>2</sup>, Anne M. Hulsey<sup>3</sup> and Kenneth J. Elwood<sup>4</sup>

(Submitted May 2024; Reviewed June 2024; Accepted July 2024)

#### **ABSTRACT**

The recent release of the 2022 national seismic hazard model has highlighted significant changes in the quantified seismic hazard for much of New Zealand that has prompted the development of draft changes to the NZS 1170.5 seismic design provisions. One proposed change is to the shape of the design spectrum, which was previously provided by a spectral shape factor,  $C_h(T)$ , that is a function of site class only. However, research has shown that spectral shape is strongly affected by several additional factors including earthquake magnitude and shaking intensity. Moreover, the use of fixed spectral shapes that vary only by site class results in significant variability between the functional form of the elastic design response spectrum, C(T), and the direct results from the national seismic hazard model. International loading standards typically include a dependency on intensity and site class in the spectral shape equations and these form the basis for the approach recommended here. The functional form of the design response spectrum is also updated to better represent spectral displacement demands on longer period structures. The proposed new spectral shape equations are compared to the 2022 national seismic hazard model output and the equations used in the previous New Zealand loading standard. Results show that the proposed approach provides a significantly better approximation of the national seismic hazard model results than the current spectral shape across a range of periods, site classes, annual probabilities of exceedance, and locations.

https://doi.org/10.5459/bnzsee.1692

#### INTRODUCTION

The recent release of the 2022 National Seismic Hazard Model (NSHM2022) has prompted re-examination of the New Zealand seismic design provisions, NZS 1170.5 [1]. In response, a Seismic Risk Work Group (SRWG) was established to propose updates to Verification Method B1/VM1, which is the primary means of demonstrating compliance with Clause B1:Structure of the New Zealand Building Code. This is a multi-year project that seeks to develop improvements to New Zealand seismic design practice, most notably updates to NZS 1170.5 [1]. A proposed Technical Specification (TS) document, TS 1170.5, expected to be released in 2024, will provide an updated methodology to determine seismic design loads for buildings. The TS incorporates the latest NSHM2022 and includes an updated method for computing the horizontal design action coefficient, C(T). This paper outlines the proposed changes to the implementation of the horizontal design action coefficient in TS 1170.5. In particular, the reasons for using site class and intensity dependent variables to represent the NSHM2022 results are presented. This paper focuses on the spectral shape provisions and forms part of a series of publications outlining relevant background information supporting the publication of the proposed TS. Refer to Lee et al. [2] and Hulsey et al. [3] for further details on site classification and risk distribution of the new hazard model respectively.

#### **Functional Form of Acceleration Response Spectra**

Shaking intensity has traditionally been parameterized in the form of smoothed, 5%-damped, elastic pseudo acceleration response spectra. Response spectra, first proposed in the 1930s

(refer to Housner [4] and Sorrentino [5]), plot a peak response quantity (e.g. acceleration, velocity, or displacement) caused by earthquake shaking as a function of the structure's natural period of vibration, T. For a specific earthquake ground motion, response spectral quantities are generated by solving the equation of motion using time-stepping integration methods [6] to give the peak displacement demand,  $S_d$ , for given values of T. Pseudo velocity,  $S_{\nu}$ , and pseudo acceleration,  $S_a$ , responses can then be obtained from Equations 1 and 2 respectively:

$$S_{\nu} = S_d \, \frac{2\pi}{T} \tag{1}$$

$$S_a = S_d \frac{4\pi^2}{T^2} \tag{2}$$

It is important to note that pseudo spectral acceleration and spectral acceleration are close except for large damping values at long periods. Furthermore, for the purpose of design, pseudo acceleration is the quantity of interest as it relates the peak displacement and base shear of a single degree of freedom oscillator [7].

During the 1970s, Newmark observed [8, 9] that many earthquake acceleration response spectra obtained from real earthquake ground motion recordings could be enveloped, in the period range important to building design, by a mathematical relationship in which for short structural periods, the maximum acceleration would be constant; for intermediate periods, the maximum velocity would be constant; and for long periods, the maximum displacement would be constant (Figure 1). The period value demarcating these constant response

<sup>&</sup>lt;sup>1</sup> Corresponding Author, Postdoctoral Fellow, University of Canterbury, Christchurch, tom.francis@canterbury.ac.nz

<sup>&</sup>lt;sup>2</sup> Professor, University of Canterbury, Christchurch, <u>timothy.sullivan@canterbury.ac.nz</u> (Member)

<sup>&</sup>lt;sup>3</sup> Research Fellow, University of Auckland, Auckland, <u>anne.hulsey@auckland.ac.nz</u>

<sup>&</sup>lt;sup>4</sup> Chief Engineer, Ministry of Business, Innovation and Employment, Wellington, <u>kenneth.elwood@mbie.govt.nz</u> (Fellow)

regions can be defined by the corner period,  $T_c$  that represents the transition from a spectral acceleration plateau to the constant spectral velocity, and the spectral displacement corner period,  $T_d$ , that defines the transition from the spectral velocity plateau to a constant value of spectral displacement demand.

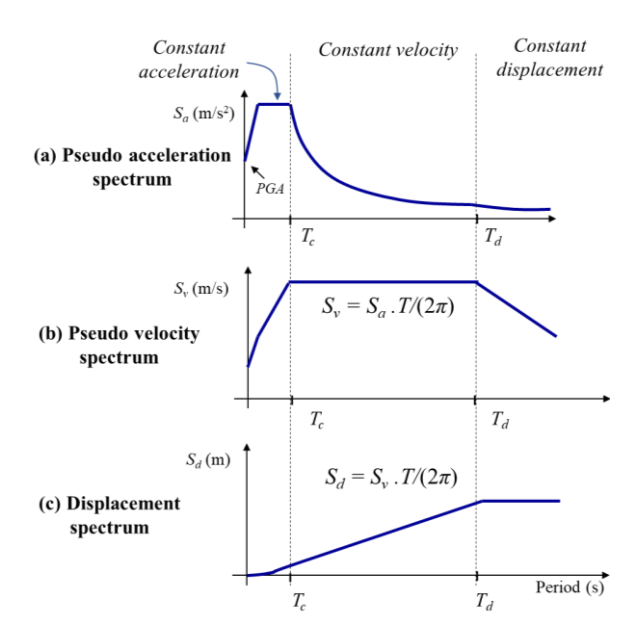


Figure 1: Newmark's traditional form of (a) pseudo acceleration response spectra, (b) pseudo velocity spectra, and (c) displacement response spectra commonly used in seismic loading standards.

#### **Factors Affecting Response Spectral Shapes**

#### Influence of Site Soil Class

The influence of site class on the response spectra shape was first noted by Hayashi et al. [10] and Kuribayashi et al. [11] who studied spectral shapes using ground motion sets of 61 and 44 records respectively. Seed et al. [12] conducted a more comprehensive study with 104 ground motion records and concluded that site conditions should be considered when defining earthquake-resistant design criteria. The site soil conditions modify the characteristics of incoming earthquake waves at bedrock, with significant amplification expected for soft soil sites but with soil non-linearity limiting the amplification in intense earthquakes. Soil amplification occurs throughout the period range, up to 10 seconds. Soft soil amplification is more pronounced at longer distances (30-50 km) for both moderate and large magnitude earthquakes [12]. The effect of site soil condition is usually accounted for in loading standards by defining site classes, with these sometimes defined in relation to the time-averaged 30 m depth shear wave velocity,  $V_{s,30}$  (e.g., ASCE 7-22 [13]). The softer the site class (lower  $V_{s,30}$ ), the wider the constant acceleration plateau.

### Influence of Earthquake Magnitude

The change of spectral shape with earthquake magnitude was first suggested in the 1970s by McGuire [14], and Trifunac and Anderson [15]. The earthquake magnitude tends to affect the long-period components of a response spectrum. Faccioli et al. [16] reported that the spectral displacement corner period ( $T_d$  in Figure 1) appears to increase almost linearly with magnitude. Additionally, there is a slight tendency for the spectral displacement corner period to increase for soft soils with large magnitude earthquakes, but this is less obvious for moderate magnitude earthquakes.

#### Shaking Intensity

Earthquake shaking intensity can affect spectral shape because higher intensity shaking can cause soil non-linearity. Furthermore, as the earthquake shaking intensity changes, so too can the magnitude and distance of the earthquake most likely to cause that shaking intensity. As magnitude and distance have been noted to affect spectral shape [17, 18, 19], it is likely that spectral shape will change for different design intensity levels. Figure 2 illustrates the impact of intensity and site class on spectral shape by considering Uniform Hazard Spectra (UHS) from the NSHM2022 for a range of TS 1170.5 site classes. Refer to Lee et al. [2] for further background on site classes in the proposed TS. For low intensity shaking, spectral accelerations tend to increase as  $V_{s,30}$  reduces, which suggests that softer soils tend to amplify the spectral accelerations throughout the period range when soils behave elastically. However, for high intensity shaking, softer soils are subjected to nonlinear deformations that limit spectral acceleration demands, whereas rock sites can sustain the stronger shaking in the elastic range, resulting in higher spectral acceleration demands for short period structures that have similar fundamental periods to the predominant period of the ground motion at a site.

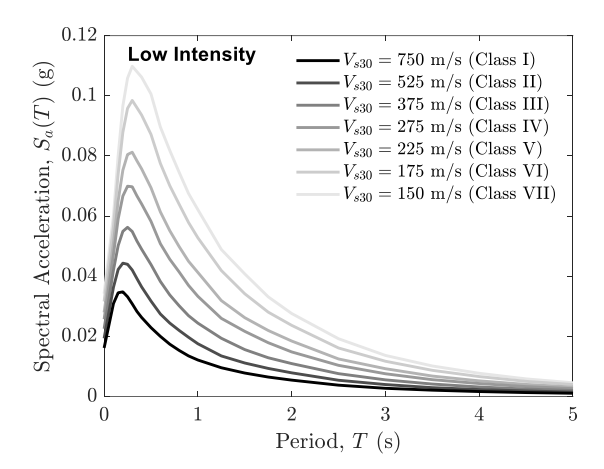
#### Near-Fault and Directivity Effects

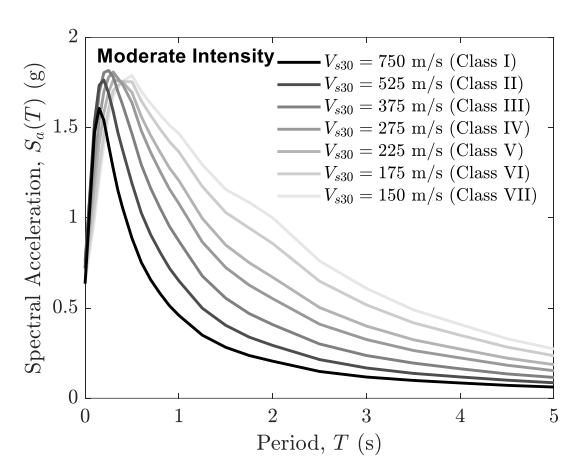
So-called "near-fault" and "directivity" effects are also known to affect the shape of response spectra. Somerville et al. [20] found that peak accelerations at sites less than 30 km from the rupture source in the 6.7  $M_w$  1994 Northridge earthquake exceeded the median value predicted by empirical attenuation relations by 50%. This finding, coinciding with similar observations from the 6.9  $M_w$  1995 Kobe Earthquake, prompted revisions to attenuation relationships [21, 22], which led to updated methods for considering near-fault and directivity effects in loading standards [23]. More recently, Weatherill [24] investigated near-fault and directivity effects specific to New Zealand Probable Seismic Hazard Analysis (PSHA).

For earthquakes that occur near a building and generate waves that propagate towards the structure, buildings that are characterised by periods of vibration close to the pulse-period of the earthquake will experience demands that are amplified (potentially by a factor of 2.0) relative to other periods. However, the hazard at a site is affected by a broad range of possible earthquake scenarios, most of which will not be characterised by near-fault effects and as such, loading standards sometimes include moderate amplification factors to allow for near-fault effects. These are also specified over a period range intended to cover the pulse period range. For example in NZS 1170.5 [1] the spectrum is amplified by a factor N(T,D) that is equal to 1.0 for periods less than 1.5 s and equal to 1.72 for periods greater than 5 s, depending on the distance, D, to the closest active fault. Refer to Bradley and Weatherill [25] for further discussion on near fault effects in New Zealand seismic hazard analysis.

#### Other Factors

There are other factors (such as faulting mechanism or local topography) that can affect the shape of response spectra, but these are not examined here as they are currently considered of secondary importance compared to the factors identified in the previous sub-sections.





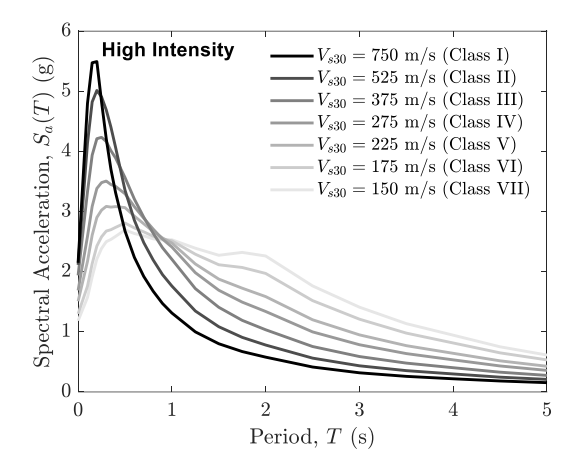


Figure 2: Spectral acceleration graphs from NSHM2022 showing the correlation between spectral shape and shaking intensity as a function of V<sub>s</sub>,30.

#### Spectral Component of Design Response Spectra

Design spectra are generated using PSHA results with ground motion prediction equations (GMPEs), typically developed using historical earthquake databases, that consider directionality effects. However, for practicality reasons it is desirable for design spectra to be represented by a single UHS where orthogonal components are inherently considered.

Several methods exist for the combination of two orthogonal components of earthquake motion for generating design spectra. NZS 1170.5 [1] spectra were derived from the work of McVerry et al. [26] who presented GMPEs based on the maximum component and geometric mean of two randomly-oriented but orthogonal horizontal ground motion components. The geometric mean spectral intensity measure [27] was commonly used in GMPEs but has the disadvantage of being

strongly dependent on the ground motion sensor orientation. This is an important consideration close to faults where directivity effects can produce strongly correlated motions [28]. To remove sensor orientation dependency, Boore [29] pioneered the use of orientation independent spectra based on the geometric-mean response spectra of two horizontal components rotated over a 90° range. Two measures were introduced, GMRotDnn and GMRotInn where "GM" stands for geometric mean, "D" stands for period dependent rotation angle, "I" stands for period independent rotation angle and "nn" is the percentile of the geometric means for all rotation angles. These approaches resulted in intensity measures that are independent of the sensor orientation but challenging to compute in practice. Boore [28] then introduced a nongeometric mean intensity measure, RotDnn, which represents the spectra obtained from a single time-series of combined orthogonal components for a range of rotation angles from 0° to 180°. The term RotD50 refers to the median spectral acceleration demand generated by a pair of recorded ground motions considering a full range of possible angles of incidence [28] while RotD100 refers to the maximum spectral acceleration demand for all angles of incidence.

In the United States (U.S.), the NGA-West2 project used RotD50 to represent design spectra for hazard analysis. However, ASCE7-22 design spectra use RotD100 and so conversion factors proposed by Shahi and Baker [30] are used to convert between the two component representations.

Furthermore, buildings generally have orthogonal lateral load resisting systems and so from a probabilistic perspective it makes sense to use RotD50 for most structures as it is unlikely that the worst case loading (i.e., RotD100) perfectly aligns with the in-plane direction of a lateral load resisting system [31]. This also means that designing buildings using RotD100 is likely to lead to discrepancies when designing to a risk target as the ground motions are likely to have a lower annual probability of exceedance (APoE) than desired [32]. For these reasons the SRWG has decided to adopt the use of RotD50 spectra within the proposed TS.

### REVIEW OF INTERNATIONAL SEISMIC PROVISIONS

#### **General Provisions**

The following subsections outline the approach taken in setting the design response spectra in the loading standards of several countries. The approaches taken can be broadly divided into several categories listed in order from simplest to most complex:

- Constant spectral shape defined for each site class, e.g., NZS 1170.5 [1].
- Spectral shape defined using a two or three parameter definition, plus scaling for site class, e.g., Eurocode 8 [33], and ASCE 7-16 [34].
- 3. Multi-period spectra, e.g., ASCE 7-22 [13].

### New Zealand - NZS1170.5:2004

NZS 1170.5 [1] defines seismic hazard and response spectra shapes with tables, maps, and equations. The general equation for the definition of elastic spectral acceleration demand, C(T), is as follows:

$$C(T) = C_h(T)ZRN(T,D)$$
(3)

where  $C_h(T)$  is a spectral shape factor (that varies according to site class), Z is the hazard factor that varies according to location across the country, R is a return period factor (with R = 1 for a 1/500 APoE) and N(T,D) is a near-fault factor that

amplifies the design response for longer periods to account for near-fault and directivity effects discussed previously.

The spectral shape factor,  $C_h(T)$ , is defined according to site class as shown in Figure 3 when using equivalent static analysis and Figure 4 for modal response spectrum and nonlinear time history analysis methods. The spectral shapes are applied for all return periods and locations, which differs from international loading standard approaches described in the next sub-sections. Figure 3 and Figure 4 also indicate that demands are lower for soil types A and B, i.e. rock sites, but Figure 2, which considers NSHM2022 data, indicates this is not true for high intensity shaking. The functional form of the design spectral shapes are made available in the NZS 1170.5 Commentary [35]. Owing to the formulation of the spectral shape equations, for periods longer than three seconds the elastic displacement response spectrum is constant (i.e.  $T_d = 3$  s).

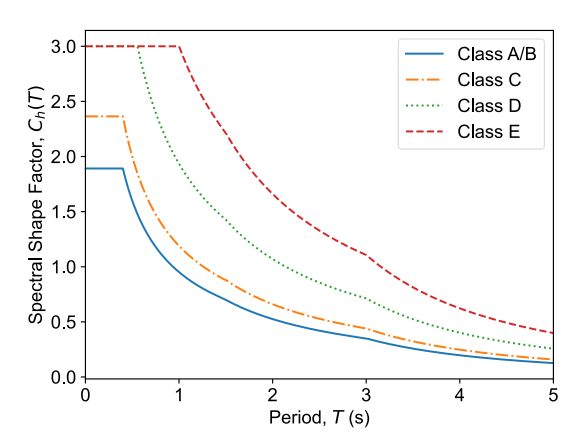


Figure 3: Standard design spectral shape, C<sub>h</sub>(T), from NZS1170.5 [1]for equivalent static analysis.

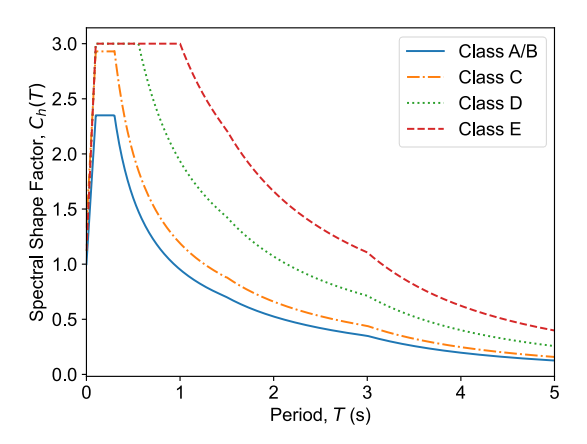


Figure 4: Spectral shape factor,  $C_h(T)$ , from NZS1170.5 [1] for modal analysis, time-history analysis, vertical loading, and parts.

#### **United States - ASCE7-22**

The U.S. approach has changed considerably over the past decade; design hazard levels are adjusted to achieve what is referred to as risk-targeted design spectra [36]. Additionally, older versions of ASCE7 defined hazard in functional form, but ASCE7-22 [13] now defines multi-period spectra (Figure 5), which directly represent the elastic spectra at each period ordinate from the U.S. NSHM according to longitude and latitude coordinates. Two-period spectra are also available (as legacy due to past familiarity) in functional form. The two-period spectra are defined by the risk-targeted Maximum

Considered Earthquake (MCE<sub>R</sub>) 5% percent damped, spectral response acceleration parameter at short periods,  $S_S$ , and at a period of one second,  $S_I$ .  $S_S$  and  $S_I$  are adjusted to account for site conditions to give the MCE<sub>R</sub> site-specific parameters of  $S_{MS}$  and  $S_{MI}$ . Figure 5 presents the site-specific MCE<sub>R</sub> spectra multiperiod and two-period formats for downtown San Francisco for site class D and risk category II structures obtained using the ASCE7 online hazard tool [37]. The constant acceleration region of the two-period spectrum is taken as 90% of the peak of the multi-period spectrum.

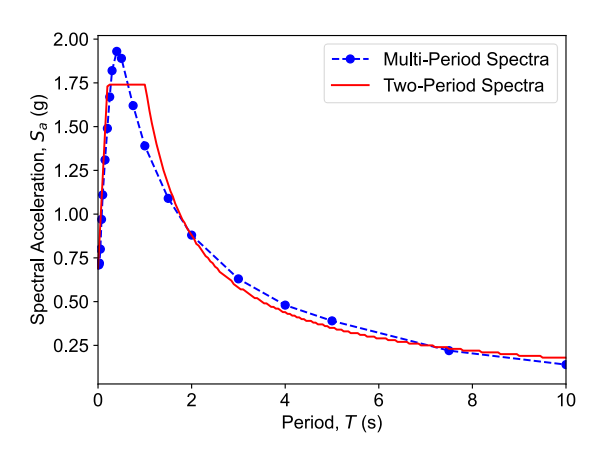


Figure 5: Example of a multi-period design spectrum and two-period design spectrum, per ASCE7-22.

The functional form of the two-period ASCE7-22 design spectra is shown in Figure 6.  $S_{DS}$  and  $S_{DI}$  represent the design level spectral ordinates accounting for site effects calculated by factoring the site specficic MCE<sub>R</sub> spectral ordinates,  $S_{MS}$  and  $S_{MI}$ , by 2/3.  $T_0$ ,  $T_S$ , and  $T_L$  represent the periods defining the beginning of the constant acceleration plateau, the end of the constant acceleration plateau, and the beginning of the constant displacement range, respectively. Owing to the formulation of the spectral shape equations (Figure 6), for periods longer than  $T_L$  the elastic displacement response spectrum is constant.

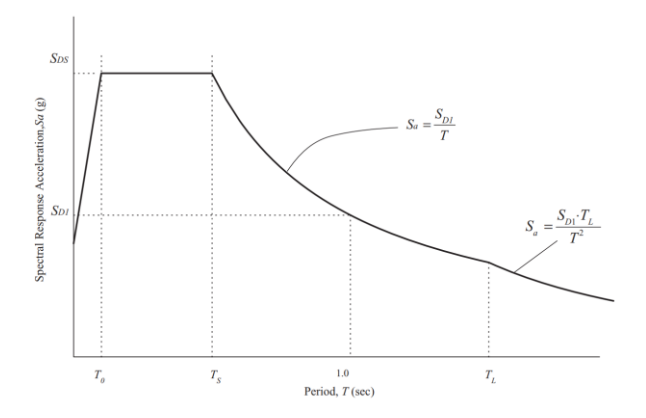


Figure 6: ASCE7-22 design response spectrum [13].

#### Europe - Eurocode 8

#### General Provisions

Eurocode 8 [33] defines a design response spectrum shape with parameters that vary according to site class and ground motion intensity. Parameters are generally set by individual territories and are listed in the relevant national annex to Eurocode 8. The general design response spectrum shape is given by:

$$S_e(T) = a_g S \left[ 1 + \frac{T}{T_B} (2.5\eta - 1) \right] \quad 0 \le T \le T_B$$
 (4a)

$$S_e(T) = 2.5a_g S \eta \qquad T_B \le T \le T_C \tag{4b}$$

$$S_{e}(T) = 2.5a_{g}S\eta \left[\frac{T_{C}}{T}\right] \qquad T_{C} \leq T \leq T_{D}$$
 (4c)

$$S_e(T) = 2.5a_g S\eta \left[ \frac{T_c T_D}{T^2} \right] \qquad T_D \le T \le 4 \text{ s}$$
 (4d)

where T is the period of vibration of a linear SDOF system,  $a_g$  is the peak ground acceleration for type A ground (the reference site class, taken as rock with  $V_{s,30} > 800$  m/s),  $T_B$  is the lower limit of the constant acceleration branch,  $T_C$  is the upper limit of the constant acceleration branch,  $T_D$  is a value that defines the beginning of the constant displacement range, S is the soil factor, and  $\eta$  is the damping correction factor. The shape of the elastic response spectrum according to Equation 4 is shown in Figure 7. Similar to the functional form of the NZS 1170.5 [1] and ASCE7-22 [34] provisions, spectral displacements are constant for long periods, i.e., for  $T > T_D$ .

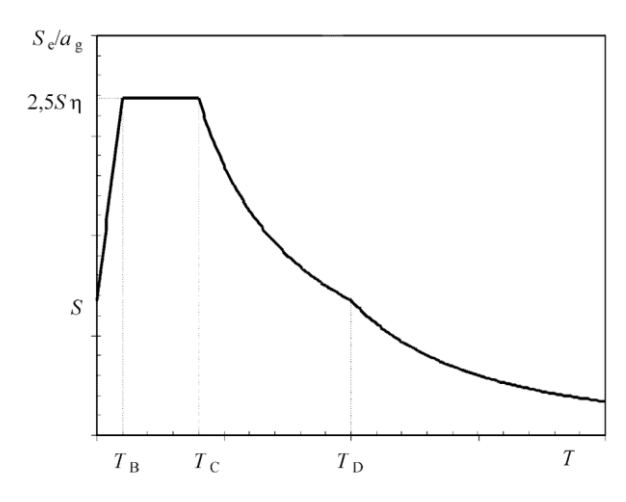


Figure 7: Shape of the Eurocode 8 elastic response spectrum adapted from Eurocode 8 [33].

The second generation of Eurocode 8 is currently under development and is expected to be released at the start of 2026 [38]. The proposed shape of the updated design spectrum is similar to the first generation and includes the feature of constant displacement for periods greater than  $T_D$ . However, the design spectrum is to be set using the two-period approach as seen in ASCE7 [13], where the constant acceleration plateau and spectral acceleration at a period of one second are defined using maps and are a function of site classification.

#### Italian Provisions

For over a decade, Italy has defined its own response spectra, in lieu of Eurocode 8, according to longitude and latitude coordinates that can be used to obtain response spectrum parameters using on-line software. Practitioners are provided with design spectral shapes fit to uniform hazard spectra, which include a peak ground acceleration,  $a_8$ , an acceleration plateau defined as a multiple of the PGA,  $a_8Fo$ , and corner period,  $T_c$ , that defines the boundary between the short period acceleration plateau and the constant velocity range of the design spectrum.

# PROPOSED TS 1170.5 ELASTIC SITE SPECTRA FOR HORIZONTAL LOADING

Different options were considered and explored for the definition of spectral shape. The proposed spectral shape was selected to be similar to traditional spectral shapes to maintain ease of use, but defined to minimise variability in risk due to the fitting process.

#### Spectral Acceleration, $S_a(T)$

The site design coefficient in the proposed TS is given by:

$$C(T) = S_a(T) \tag{5}$$

where the spectral acceleration,  $S_a(T)$ , shown in Figure 8 and obtained from Equations (6a) to (6d), is a simplified representation of the UHS at the defined APoE for RotD50 pseudo acceleration demands on SDOF oscillators characterised with period, T, and 5% damping. The use of RotD50 spectra is a departure from NZS 1170.5 [1] and aims to better represent the risk associated with the direct PSHA results. The proposed functional form of the spectral acceleration is given by Equation 6 and illustrated in Figure 8:

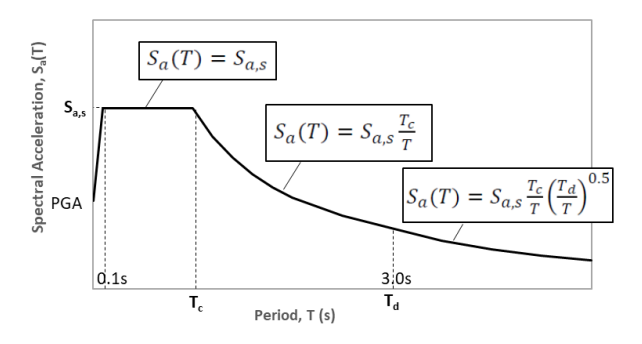


Figure 8: Functional form of the proposed spectral shape equations.

$$S_a(T) = PGA$$
 for  $T = 0$  s (6a)

$$S_a(T) = S_{a,s}$$
 for 0.1 s \le T < T\_c (6b)

$$S_a(T) = S_{a,s} \frac{T_c}{T} \qquad \text{for } T_c \le T < T_d$$
 (6c)

$$S_a(T) = S_{a,s} \frac{T_c}{T} \left(\frac{T_d}{T}\right)^{0.5} \quad \text{for } T_d \le T$$
 (6d)

Equation (6a) indicates that for rigid systems with T=0 s, the spectral acceleration should be considered equal to the peak ground acceleration taken directly from the UHS. For structures with period between 0 s and 0.1 s, the demand is set equal to  $S_{a,s}$  if the equivalent static method is adopted, but linear interpolation between PGA and  $S_{a,s}$  may be used for other structural analysis methods. The intention of this clause is to recognise that if the structural period of vibration is estimated to be less than 0.1 s via the equivalent static method, then owing to uncertainties in period estimates, it may be non-conservative to design for demands lower than  $S_{a,s}$ . However, it is also considered reasonable to assume that demands on higher modes of vibration with very short periods may be less than  $S_{a,s}$ .

Equation (6b) indicates that for short-period structures possessing periods between 0.1s and a period  $T_c$  (defined as a function of APoE, site class and location) a constant value of  $S_a(T)$ , equal to  $S_{a,s}$ , should be assumed. The value of  $S_a$  from the NSHM2022 UHS in line with historical representations of

demand and similar approaches used internationally (such as in ASCE7-22). The definition of a constant value of  $S_{a,s}$  in the short period range is considered advantageous from a design perspective to avoid fluctuation in the design forces with period for simple short period structures.

Equation (6c) indicates that for SDOF systems with period between  $T_c$  and  $T_d$ , spectral acceleration demands reduce in proportion to 1/T. Consistent with Newmark's traditional design spectrum functional form (Figure 1), this period range is characterised by reasonably uniform spectral velocity demands. Equation (6d) indicates that beyond a spectral velocity plateau corner period,  $T_d$ , the acceleration demands reduce more quickly with T than they do within the uniform spectral velocity region. The equation also implies that UHS spectral displacement demands will continue to increase beyond the period  $T_d$ , but at a slower rate of increase than in the uniform spectral velocity region.

Faccioli et al. [16] have shown that  $T_d$  should be considered a function of earthquake magnitude, and that displacement demands will tend to plateau beyond this point. However, due to the contribution of a wide range of magnitudes and source-to-site distances to the hazard at any given location, a distinct spectral displacement plateau is not typically observed in the NSHM2022 UHS. Moreover, when evaluating UHS shapes derived from NSHM2022, it was found that the functional form of the spectrum provided by Equation 6 could adequately represent the UHS shape for most sites out to periods of approximately six seconds, as the spectral shape equations allow for some continued increase in spectral displacement beyond  $T_d$ , thereby allowing for the range of earthquake magnitudes that can influence the demands at long periods.

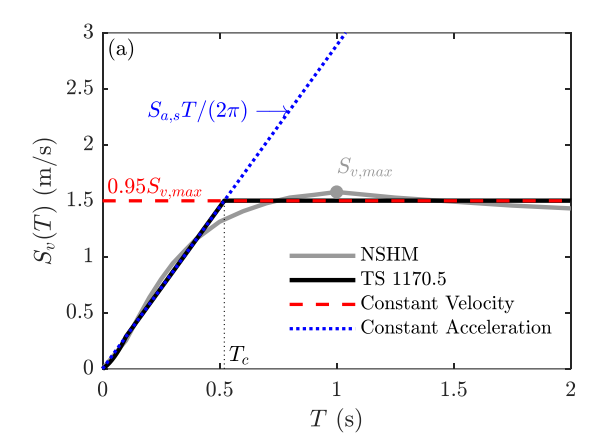
Initially, the SRWG recommended the use of Equation 6(d) with a fixed value of  $T_d = 3$  s, but this approach proved overly conservative for some locations, particularly where a least-squares fitted  $T_d$  value below three seconds provided a better match to the data. As a result, the SRWG concluded that it is more appropriate to fit  $T_d$  individually for each site and APoE. The implications of selecting a fixed  $T_d$  as opposed to fitting each individual spectra with a unique  $T_d$  obtained by least squares regression is discussed later, including the implications for the design of long-period structures that may previously have been non-conservatively represented owing to the spectral shape definitions in NZS 1170.5 [1]. The resulting spectral shape is expected to provide an increasingly conservative representation of UHS demands for periods greater than six seconds.

#### Removal of the Near Fault Factor, N(T,D)

The strength and duration of earthquake ground-motions within a few kilometres of the earthquake rupture surface are strongly influenced by several near-fault effects producing features that are not generally present in motions at sites more distant from the rupture. Such effects are accounted for in a rupture-averaged sense in the underlying NSHM2022 [25].

A recent study undertaken by Weatherill [24] examined the topic of directivity effects and observed that the current nearfault factors are considered to be conservative in relation to the mean hazard from NSHM2022, particularly at long periods, and could be reduced. After trialling a PSHA approach in which uncertainty in hypocentre location and the influence of multiple sources close to a fault are accounted for, Weatherill [24] found that for most of New Zealand the design accelerations would increase by less than 5-10% relative to the PSHA results without consideration of these effects (demonstrating that the near fault factors are conservative). In addition, Weatherill [24] points out that if the full Wellington fault triggers, there is likely to be no near-fault effect because Wellington city is located over the centre of the fault. During SRWG discussions, concern was raised about the chance that a near-fault earthquake does

occur with higher amplification. However, because faults with near-fault effects are considered in the NSHM2022, and spectral demands for some locations such as Wellington are already high, the SRWG decided to remove the near fault factor in the proposed TS. Furthermore, the addition of a near-fault factor implies that sites close to fault-lines are subjected to a greater rupture-average hazard compared to sites further afield which is inconsistent with an intention of the TS to provide design spectra that are uniform in hazard throughout the country.



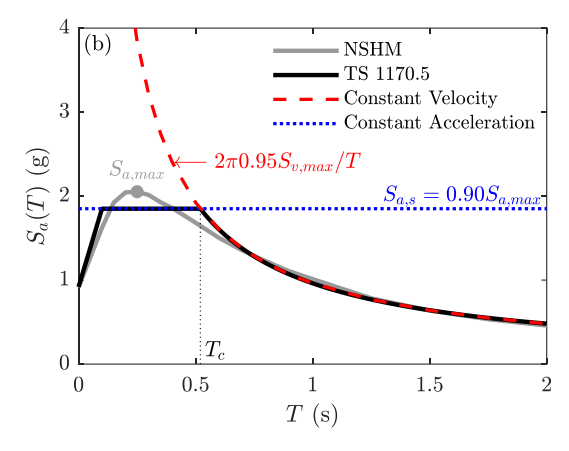


Figure 9: Procedure adopted to fit spectral shape equations to UHS from the NSHM2022 in (a) spectral velocity ordinates and (b) spectral acceleration ordinates.

# Fitting the Proposed Functional Form to the Uniform Hazard Spectra

The design spectral acceleration  $S_a(T)$  is defined for all site classes and APoE using the variables: PGA,  $S_{a.s.}$ ,  $T_c$  and  $T_d$ . The design spectra was fit to the mean UHS from NSHM2022 (except for the top of the north Island, including Auckland, where a floor was introduced, as discussed later in this paper). PGA is obtained directly from NSHM2022 while  $S_{a.s.}$  is set to be equal to 90% of the peak spectral acceleration across all considered periods,  $S_{a,max}$ . The spectral acceleration corner period,  $T_c$ , is set by:

$$T_c = \frac{2\pi (0.95S_{v,\text{max}})}{S_{a,s}} \tag{7}$$

where  $S_{v,max}$  is the peak spectral velocity obtained directly from the NSHM2022. The expression for  $T_c$  in Equation (7) was obtained by solving for the period ordinate that represents the intersection of the constant acceleration and constant velocity portion of the UHS which is shown graphically in Figure 9(a) and Figure 9(b) for spectral velocity and spectral acceleration ordinates, respectively.  $T_c$  values are rounded to two significant

figures as opposed to two decimal places which provides the best fit in the constant velocity range without the implied accuracy associated with providing more precise  $T_c$  values above one second.

 $T_d$  was obtained via least-squares regression to minimise the difference between the NSHM2022 UHS and the design spectral acceleration values,  $S_a(T)$ , for period ordinates between  $T_c+0.5$  s and six seconds (inclusive). This period range was selected to ensure design spectra accurately represent the NSHM in the period range applicable to most structures, despite NSHM results being reported for periods up to 10 s. The minimum displacement corner period was set as  $T_c+0.5$  s to recognise that the constant acceleration corner period,  $T_c$ , may sometimes exceed this value for high intensity, soft soil sites at locations where the hazard is dominated by large magnitude shaking. Periods longer than six seconds were not considered

for regression owing to the very small number of structures characterised by periods in this range.

An example of the fit offered by Equation (6) is shown in Figure 10 for a selection of the NSHM2022 spectra in Figure 2. Several site classes (refer Lee et al. [2]) have been omitted for clarity to show the ability of Equation (6) to match the NSHM2022 results across a range of intensities. Alternatively, Figure 10 can be considered to represent the fit offered across the range of return periods used for design at a single site. The functional form in the proposed TS provides a close fit to the NSHM2022 across the period range considered, particularly for medium and high-intensity design spectra. The performance of the fitted approach is evaluated more thoroughly in the section, Evaluating the Suitability of the Recommended Spectral Shape Approach.

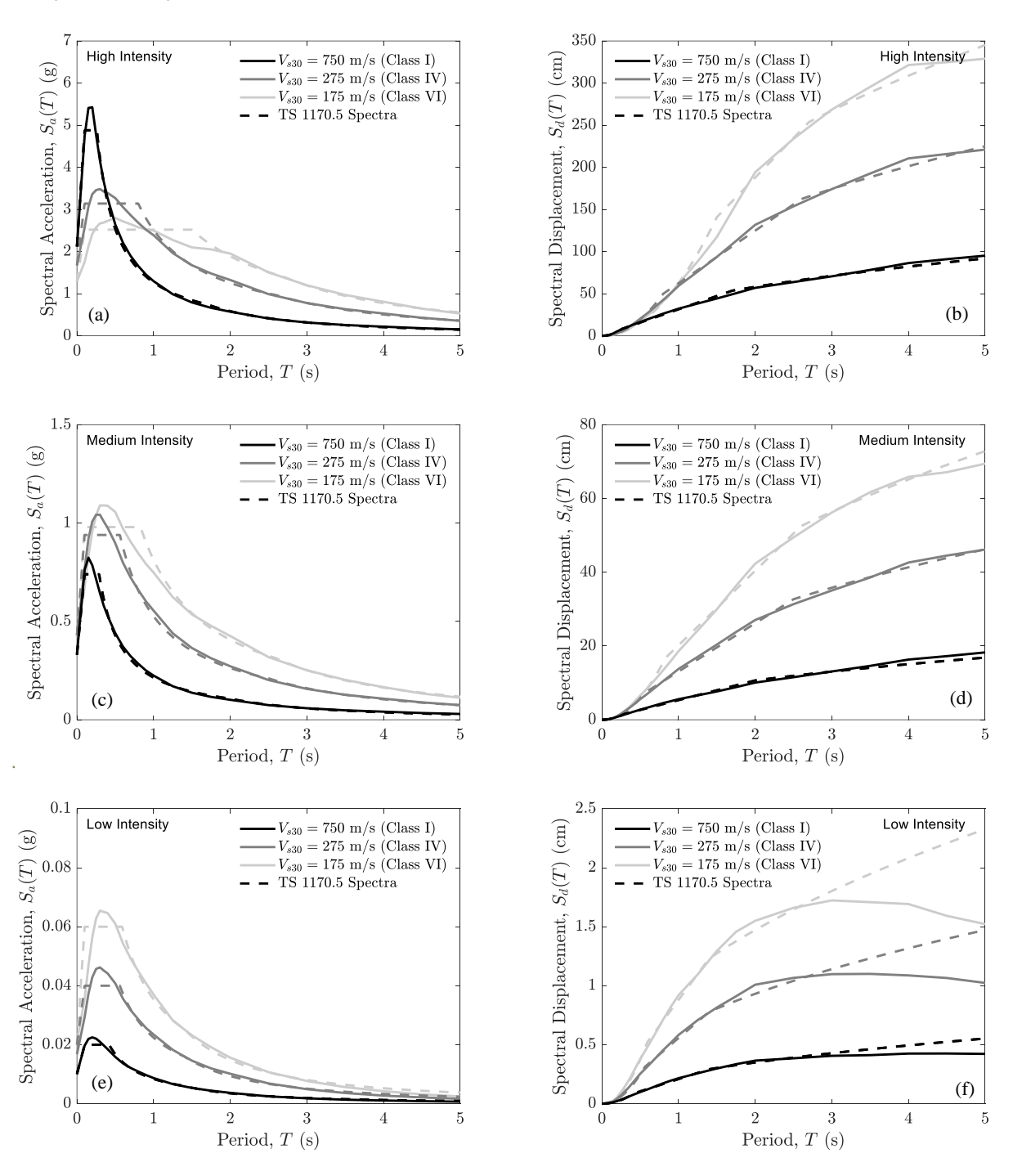


Figure 10: Example of the fit offered by Equation (4) (dashed lines) to the NSHM2022 results across spectra representing a broad range of design intensities and site classifications.

#### Obtaining Parameters for Lower-Bound Design Spectra

Hulsey et al. [3] discuss the introduction of a lower-bound design spectrum for low-seismicity sites in northern New Zealand. The lower-bound is based on the 90<sup>th</sup> percentile spectra obtained for Auckland and ensures that building designs anywhere in New Zealand comply with a minimum level of earthquake-shaking intensity. Design parameters were initially derived using both the local mean spectrum and the Auckland 90th percentile spectrum, identified with the subscripts *mean* and *akl90* in Figure 11. The method used to fit these parameters to the lower-bound spectrum is also illustrated in Figure 11.

To determine  $T_d$ , the peak spectral velocity values from both the local mean and Auckland 90th percentile spectra are compared. If the Auckland 90th percentile spectral velocity exceeds the local mean,  $T_d$  is taken as the maximum of the two corresponding  $T_d$  values. Otherwise, the  $T_d$  from the local mean spectrum is used. This approach ensures that, for periods greater than  $T_d$ , the design spectrum calculated using the code equations will always exceed the Auckland 90th percentile spectrum, providing a conservative design envelope.

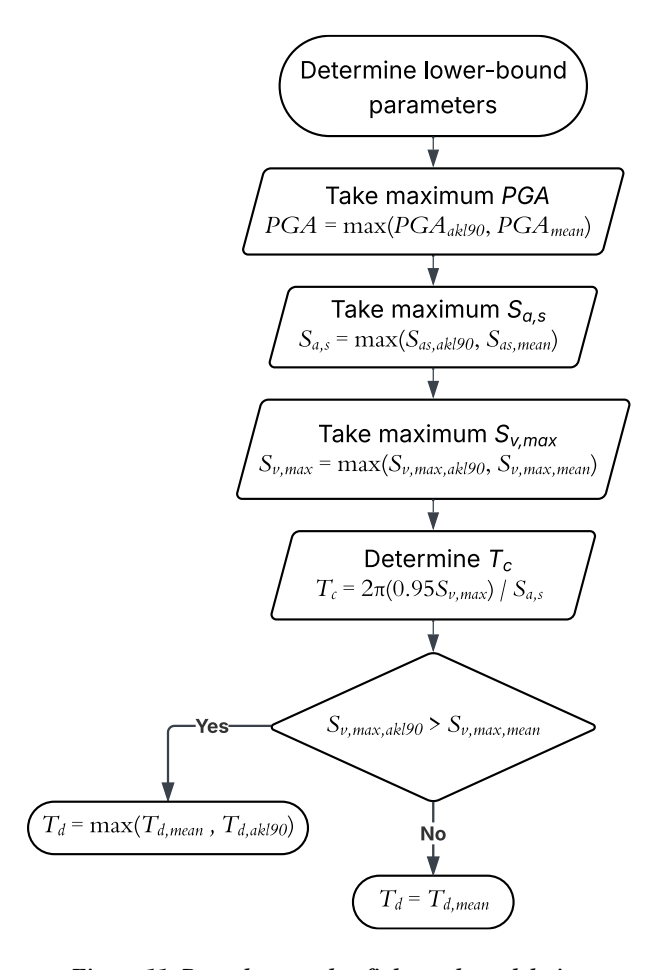


Figure 11. Procedure used to fit lower-bound design spectrum parameters.

# EXAMINING VARIABILITY IN THE SPECTRAL ACCELERATION PLATEAU CORNER PERIOD, $T_c$

### Variation with Site Class and Intensity

Figure 12 illustrates the variability of the spectral acceleration corner period,  $T_c$ , as a function of intensity (represented by the short period spectral acceleration,  $S_{a,s}$ ) and site class. Results are shown considering the mean UHS for 12 main centres (see Figure 14 for the list of cities) around New Zealand that were initially considered by the SRWG as being broadly

representative of New Zealand's seismic environment. The relationship between  $T_c$  and intensity can be approximated by a linear trend. For sites characterised by high  $V_{s30}$  values (i.e., site classes I to III),  $T_c$  is constant. In contrast, for soft soil sites,  $T_c$  increases with shaking intensity. This implies that adopting a single corner period, as done in NZS 1170.5 [1], would introduce significant discrepancies between the functional form of the elastic site demand compared to the direct NSHM2022 results. Consequently, accounting for the variation of  $T_c$  with ground motion intensity and site class was deemed necessary.

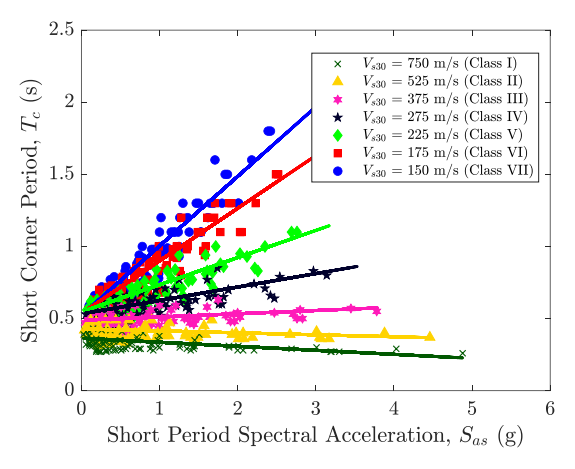


Figure 12: Illustrating variation in the spectral acceleration plateau period,  $T_c$ , as a function of intensity (represented by  $S_{as}$ ) and site class (represented by  $V_{s,30}$ ).

#### Variation with Location

Figure 13 compares spectral acceleration at different locations in New Zealand for cases where site class is identical and  $S_{a,s}$  values are very similar but  $T_c$  values differ. The figure indicates that different locations can have quite different spectral shapes for identical soil class and peak spectral acceleration,  $S_{a,s}$ . The reason for this can in part be attributed to faulting and magnitude characteristics for each site when undertaking PSHA. Sites where the design seismicity is more heavily dominated by larger magnitude shaking are likely to exhibit longer corner periods as the ground motions from this type of hazard are known to affect higher periods compared with lower magnitude, near-field shaking. This result provides further justification for the definition of spectral shapes that vary from location to location instead of varying only with intensity.

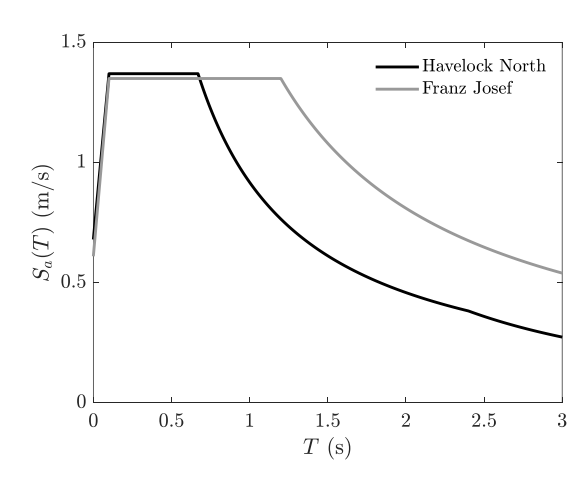


Figure 13: Comparison of 1/500 APoE, site class V acceleration response spectra for Havelock North and Franz Josef to illustrate variability in  $T_c$  according to location.

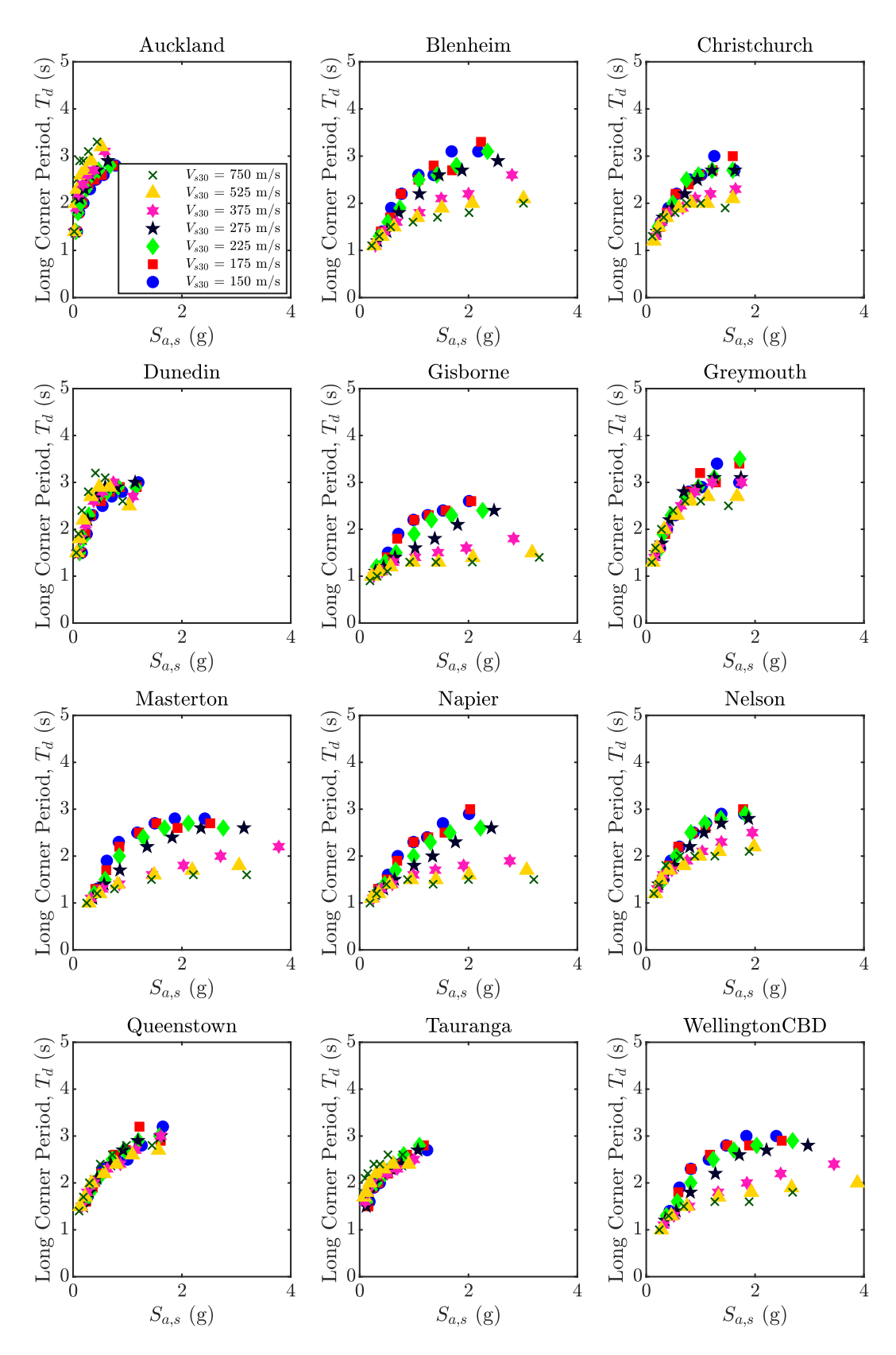


Figure 14: Illustrating the variability in fitted  $T_d$  as a function of  $V_{s,30}$  and intensity.

# EXAMINING VARIABILITY IN THE SPECTRAL VELOCITY PLATEAU CORNER PERIOD, $T_d$

#### Variation with Site Class and Intensity

The proposed TS fits  $T_d$  using least-squares regression to improve accuracy. However, a simplified approach using a single value of  $T_d = 3$  s was also considered. To examine the

implications of this, Figure 14 outlines the fitted  $T_d$  values for 12 main New Zealand centres for each considered site class and APoE. The fitted values of  $T_d$  are generally between one and three seconds. Unlike  $T_c$ , where there is a clear linear relationship with intensity as a function of soil class, fitted  $T_d$  values are significantly more varied with differences appearing to be dependent on a number of factors such as intensity and the magnitude of earthquakes affecting the site.

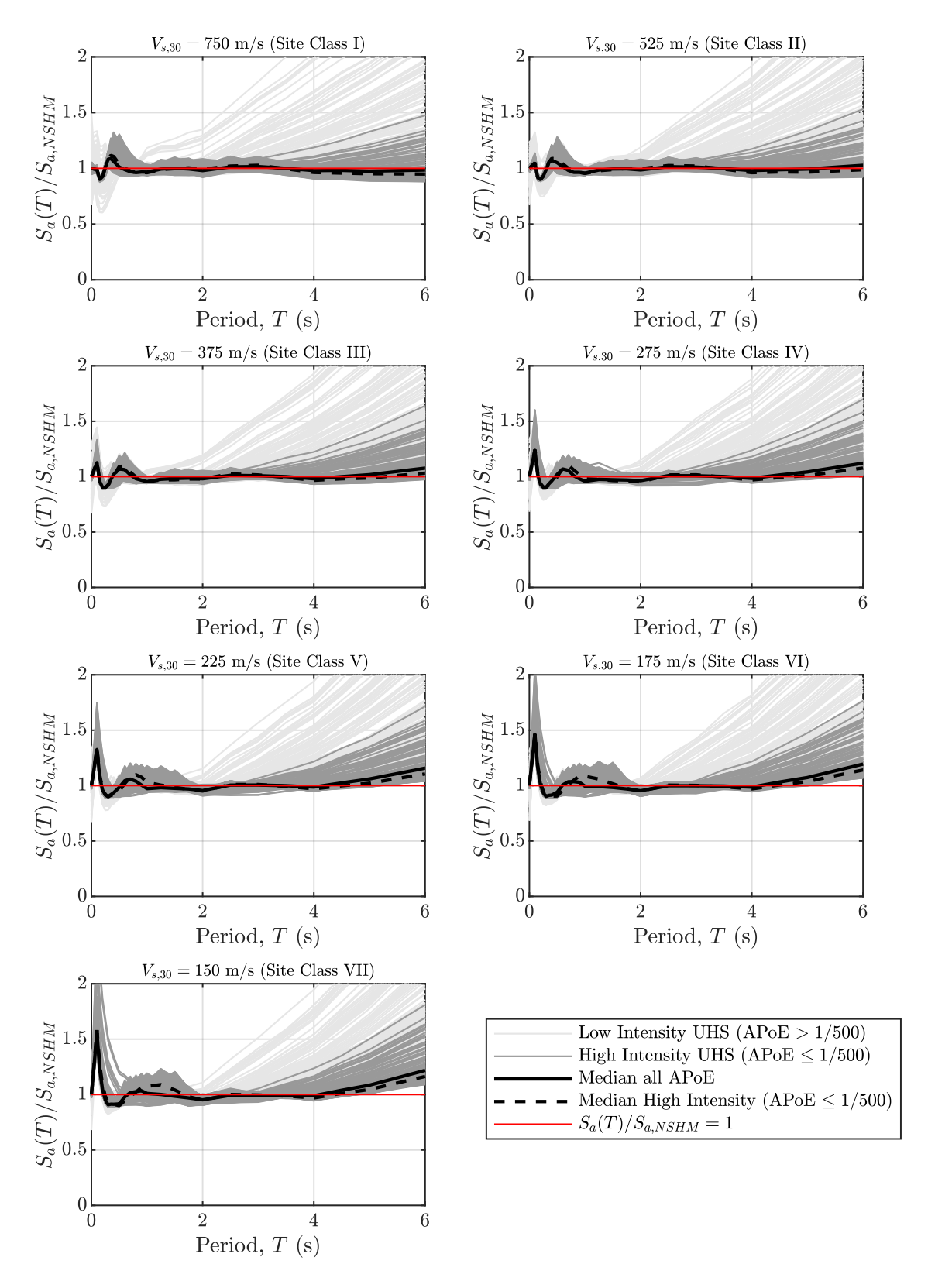


Figure 15: Illustrating the ratio of elastic spectral demands between TS 1170.5 to the direct NSHM2022 results considering the use of  $T_d$  fitted using least squares regression.

# EVALUATING THE SUITABILITY OF THE RECOMMENDED SPECTRAL SHAPE APPROACH

### Evaluating the Suitability of a Constant $T_d = 3$ s

The previous section outlined the variability in fitted  $T_d$  values obtained using least-squares regression which the SRWG

decided was preferred to using a single value of  $T_d$  for all spectra. The implications of this decision are evaluated further in Figure 15 and Figure 16 which plot the design spectrum ratio, defined as the ratio of the proposed TS design spectra,  $S_a(T)$ , to the NSHM2022 spectra,  $S_{a,NSHM}$ , for all 214 listed site locations, site classes, and APoE in the proposed TS. Figure 15 shows the design spectrum ratios for  $T_d$  fitted using least squares

regression, while Figure 16 plots results for spectra with  $T_d = 3$  s. The design spectrum ratios are grouped by high and low intensity with high intensity defined as shaking with an APoE of 1/500 years or less. Considering high intensity spectra, fitting  $T_d$  using least squares regression results in the best fit

throughout the period range of interest (0 - 6 s). Setting  $T_d$  = 3.0 s also results in reasonable accuracy with more conservatism as evidenced by the median design spectrum ratio for high intensity UHS being greater than one.

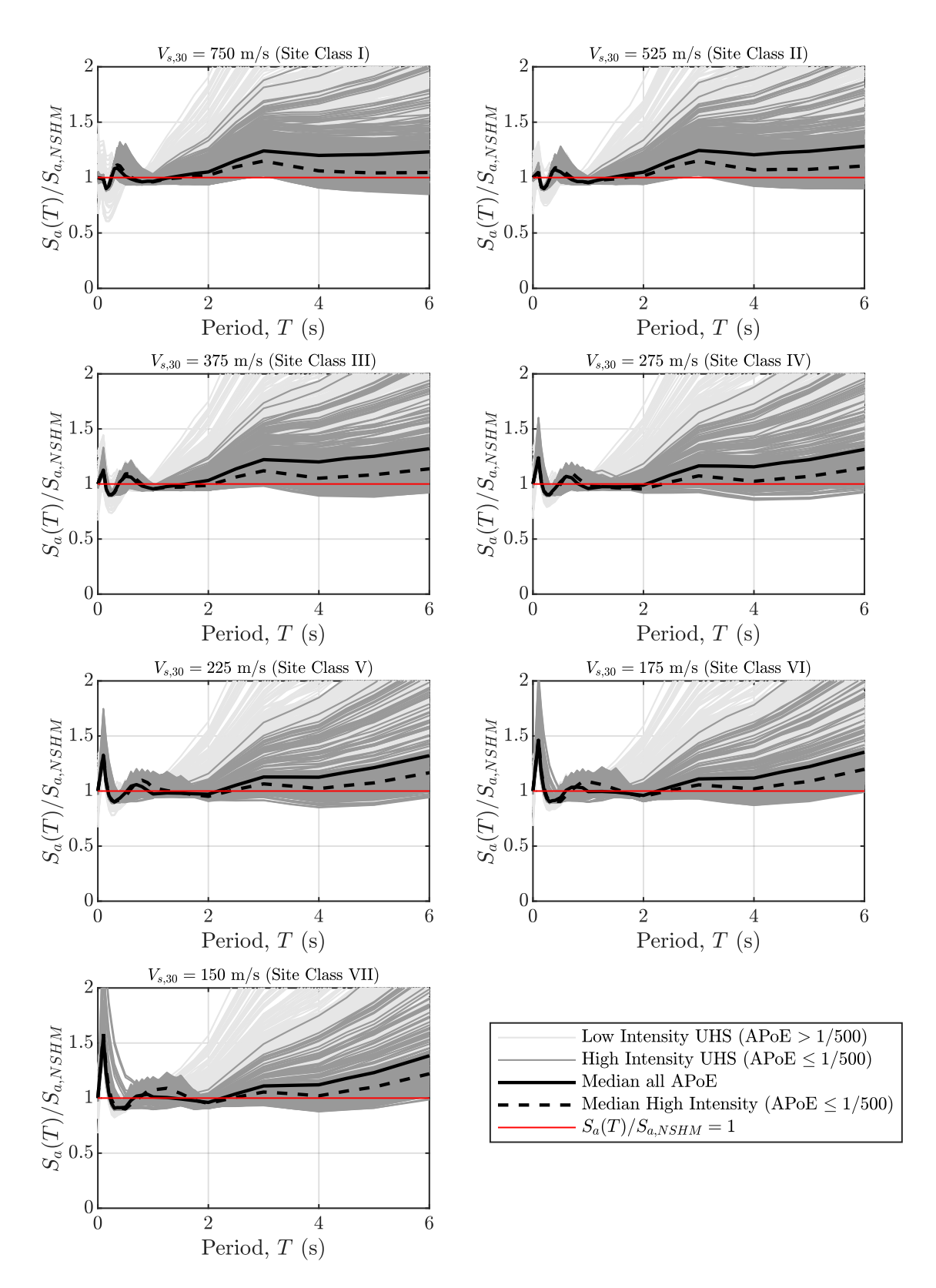


Figure 16: Illustrating the ratio of elastic spectral demands between TS 1170.5 to the direct NSHM2022 results considering the use of a constant  $T_d = 3$  s.

Note the results in Figure 15 and Figure 16 are identical for  $T < T_c + 0.5$  s which was the minimum period considered when fitting  $T_d$  using least squares regression. For very short periods, (i.e., less than 0.2 s) the design spectrum ratio can be high, particularly for sites characterized by soft soils, which is due to the period ordinate of 0.1 s used to define the start of the constant acceleration plateau. Some international loading standards minimise this error by introducing another variable to define the start of the spectral acceleration plateau, i.e.  $T_B$  in Eurocode 8 [33]. However, for design in New Zealand there is little benefit in using this additional variable as many buildings in the short period range are designed using the equivalent static method which extends the constant acceleration portion of the design spectrum back to the zero second period ordinate.

#### Fit for Low Intensity Spectra

In both the fitted (Figure 15) and constant (Figure 16)  $T_d$  cases, the conservatism in the long period range for high APoE (low intensity UHS) is caused by the fact that lower intensity displacement spectra tend to plateau at shorter periods but spectral displacement demands from Equation (6) continue to increase. For example, see Figure 10(f) where the approximate spectral displacement corner period (where displacement demands plateau) is 3 s resulting in the TS spectrum overestimating the demand for T > 3 s. While the ratio of  $S_a(T)$  to  $S_{a,NSHM}$  appears to be high for low intensity UHS at long periods, it is important to realise that the absolute demands are still very low. Different spectral shapes were considered in the long period range that would be a function of the UHS intensity, but the SRWG decided that it was preferable to use a single shape to maintain simplicity.

#### **Spectral Shape Fit for Long Periods**

Newmark [8] initially proposed the idea of constant displacement at longer periods (Figure 1) and this approach has generally been applied in international loading standards, including NZS 1170.5 [1]. However, the research of Faccioli et al. [16] highlighted that for individual displacement spectra, the period at which spectral displacement demands plateau increases as magnitude increases for  $M_w > 6.5$ . Larger rupture distances were also shown to moderately increase the long corner period for  $M_w < 6.5$ . As UHS are developed for a range of different earthquake magnitude and distances that may impact a site, the UHS spectral displacement demands do not tend to exhibit distinct spectral displacement plateaus, particularly for low APoEs. Consequently, a key characteristic of the spectral shapes in the proposed TS is that spectral displacement demands continue to increase for periods longer than  $T_d$ , which allows for a more reasonable estimation of UHS elastic demands at longer periods, as shown in Figure 17 for Wellington CBD and Christchurch for site class III. Clearly in this example, assuming constant elastic displacement demands for  $T > T_d = 3$  s would underpredict the results of the NSHM. This feature of the proposed spectral shape is important for setting realistic design parameters for long period structures, such as base isolated buildings and bridges. The SRWG also investigated the use of constant  $T_d$  values including 2 and 2.5 seconds. However, the resulting functional forms of the UHS were non-conservative for higher intensities.

#### Improvement in Normalised Spectral Shape

In NZS 1170.5 [1], design spectra are normalised at a single period ordinate of 0.5 s. Scaling is then done by a hazard factor, *Z*, which represents 0.5 times the magnitude weighted 5% damped response spectrum acceleration for a 0.5 s period for site class C with a return period of 500 years [35].

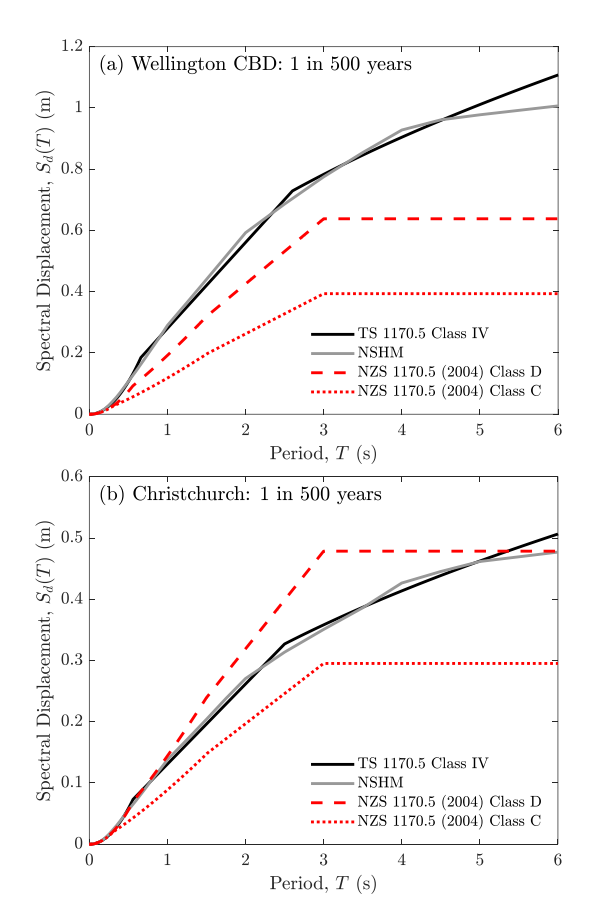


Figure 17: Illustrating typical shape of displacement response spectra (a) Wellington APoE 1/500 years site class III, (b) Christchurch APoE 1/500 years site class III.

The variability in spectral shape from normalising the NSHM2022 UHS at a single period ordinate with a hazard factor based on a single site class and APoE (i.e., the NZS 1170.5 [1] approach) is shown in the left-hand subplots of Figure 19. The normalised UHS are shown for four main centres, three APoEs (1/50, 1/500, and 1/2500), and TS site classes I, III and V. The horizontal axes of the left-hand subplots in Figure 19 are normalised by  $T_c$ , which was calculated for each site class by first obtaining the median normalised 1/500 APoE spectrum across all listed sites, then applying Equation (7). The resulting  $T_c$  values were found to be 0.3 s, 0.5 s and 0.9 s for site classes I, III, and V, respectively. This approach replicates how a single  $T_c$  value could be assigned for each site class, as is done in NZS 1170.5 [1]. NZS 1170.5 [1] corner period values were not used in this comparison due to issues in mapping the old site class definitions to those in the proposed TS.

The right-hand subplots of Figure 19 represent variability in spectral shape using the normalisation approach considered in the proposed TS, where normalisation occurs at the  $S_{a,s}$  ordinate for intensity scaling and  $T_c$  for period scaling. Although scaling is also done at the PGA ordinate, this is not considered in Figure 19 for simplicity, because the normalisation shown is applied directly to the NSHM2022 UHS instead of the codified equations. Unlike the NZS 1170.5 [1] approach, the proposed TS scales each UHS using unique values of  $S_{a,s}$  and  $T_c$ . The benefit of scaling individual spectra is clearly shown by the right-hand subplots in Figure 19 which exhibit greatly reduced variability in normalised spectral shape, resulting in a more uniform distribution of hazard throughout the country. Note that the use of multi-period spectra would result in a single line in these figures.

Furthermore, Figure 19 (left) illustrates the variability in spectral shape introduced using the return period factor, R. In NZS 1170.5 [1], the return period factor represents a generalised hazard curve for spectral acceleration with a period of 0.5 s. A single curve shape is used to represent all locations, periods, and site classes. The proposed TS approach instead defines parameters for each APoE and so a return period factor is not required, meaning the NSHM hazard curve for each location is better represented. Figure 18 shows normalised 0.5 s spectral acceleration hazard curves for Auckland, Wellington, Christchurch, and Dunedin obtained from NSHM2022 for each site class. The R-factor from NZS 1170.5 [1] is also shown and indicates that for an APoE other than 1/500 years there is a significant spread in normalised hazard curve shape. This demonstrates the limitations of using a single hazard curve shape to represent seismic demands across diverse locations and supports the preference for the proposed TS approach.

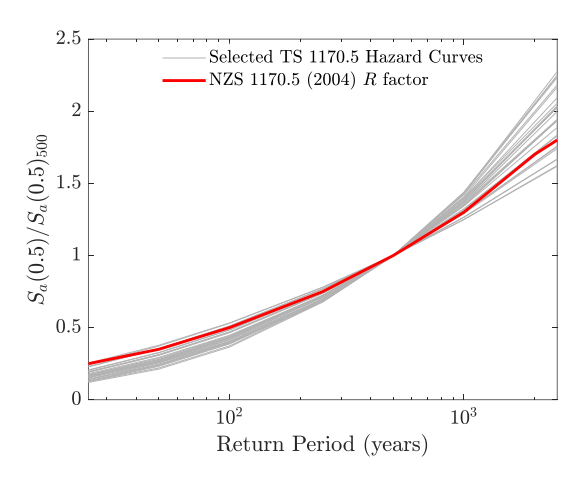


Figure 18: Selected hazard curves from TS 1170.5 compared to the NZS 1170.5 [1] R-factor.

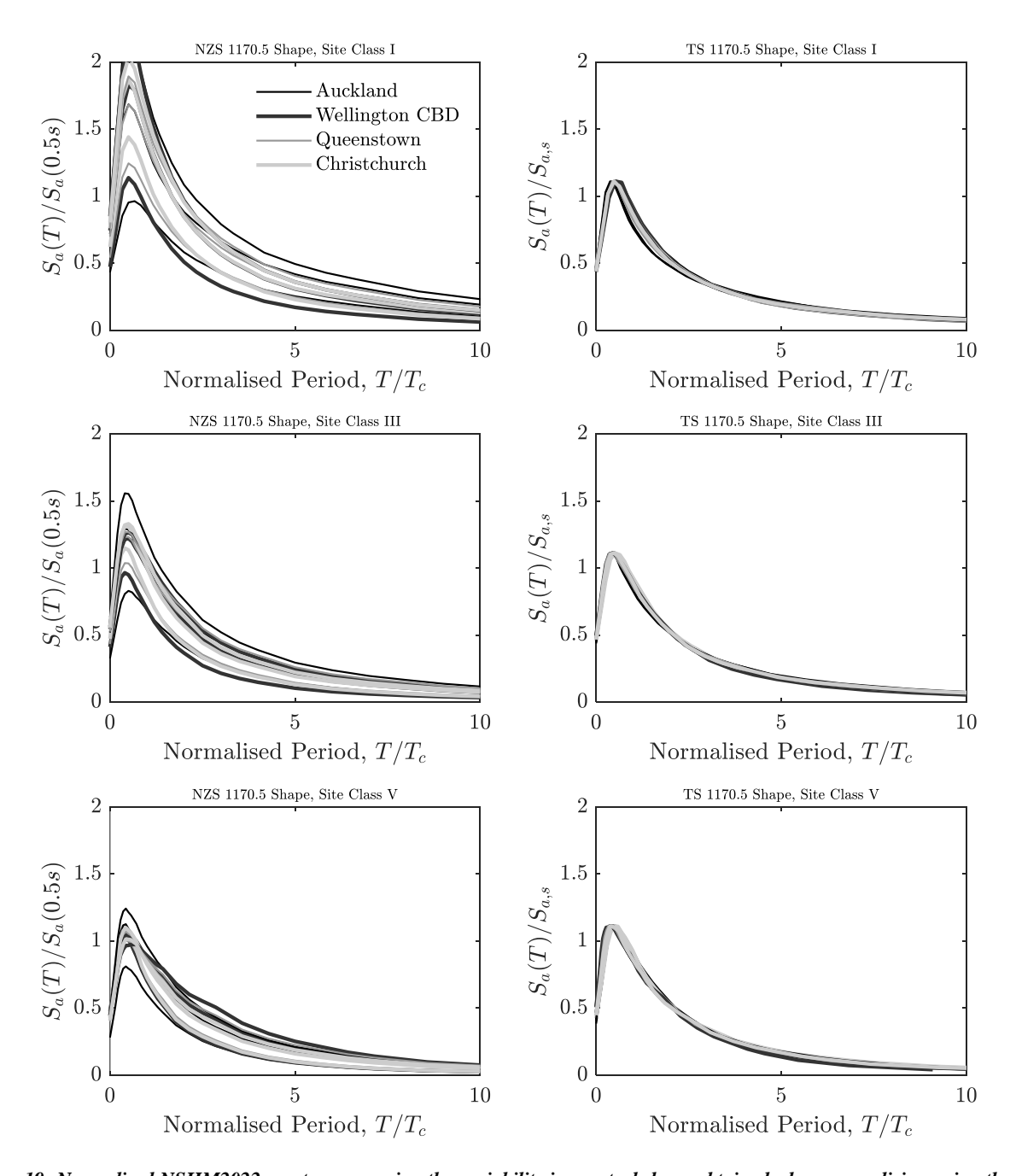


Figure 19: Normalised NSHM2022 spectra comparing the variability in spectral shape obtained when normalising using the NZS 1170.5 [1] approach (left) versus the approach used in the proposed TS (right).

M D PGA Tc  $T_{\rm d}$ PGA  $S_{a,s}$ Tc PGA S<sub>a,s</sub>  $T_{\rm c}$ Tc PGA Tc APOE Sas  $T_d$ Td PGA Sa,s  $T_d$ PGA Sa,s Tc  $T_{d}$  $S_{a,s}$  $T_d$ 1/25 6.5 n/a 0.07 0.15 0.29 1.2 0.08 0.18 0.34 1.2 0.1 0.21 0.39 1.2 0.11 0.24 0.45 1.3 0.11 0.27 0.47 1.3 0.12 0.3 0.53 1.4 1/50 6.7 n/a 0.11 0.25 0.29 1.3 0.13 0.29 0.34 1.4 0.15 0.33 0.41 1.3 0.17 0.38 0.46 1.4 0.17 0.4 0.52 1.4 0.18 0.45 0.56 1.6 1/100 6.8 n/a 0.18 0.39 0.29 1.5 0.21 0.45 0.36 1.3 0.23 0.5 0.43 1.4 0.24 0.55 0.5 1.5 0.23 0.58 0.55 1.7 0.24 0.62 0.62 1.8 1/250 7.0 n/a 0.3 0.66 0.31 1.5 0.34 0.75 0.37 1.5 0.37 0.81 0.46 1.6 0.37 0.85 0.55 1.8 0.34 0.87 0.62 2 0.35 0.89 0.73 2.2 Settlement name 7.1 >20 0.43 0.95 0.32 1.6 0.48 1.06 0.39 1.6 0.52 1.11 0.5 1.7 0.48 1.13 0.6 2.1 0.43 1.13 0.69 2.3 0.44 1.13 0.87 2.4 1/500 0.33 1.45 1.8 0.69 1.49 0.53 1.48 0.65 1.44 0.8 2.7 7.2 >20 0.59 1.33 1.6 0.66 0.41 1.9 0.62 2.4 0.54 2.5 0.54 1.42 1/1000 0.34 0.44 1.8 0.98 0.57 0.74 0.69 0.94 7.3 >20 0.87 1.98 1.8 0.96 2.13 2.12 2.2 0.83 2.03 2.7 1.94 2.7 0.68 1.89 1.2 2.9 1/2500

Table 1. Excerpt from TS 1170.5 Table 3.4 showing site demand parameters.

#### **Considering the Ease of Implementation**

One design table for each APoE is provided in the proposed TS, for which an excerpt is shown in Table 1 for the 1/500 APoE. Each table outlines all parameters required to fully define the elastic spectral acceleration in Equation (6) for site classes I-VI. Additionally, the earthquake magnitude, M, for each site and APoE is provided. While this approach requires the tabulation of further data than was necessary in NZS 1170.5 [1], the SRWG considers that the improvements in fit offered by the new spectral shape approach justifies the need for additional data

#### CONCLUSIONS

This paper presents a review of international seismic design provisions as they relate to spectral shape and outlines the reasoning for the proposed spectral shape provisions in TS 1170.5. The equations that specify the spectral shape in the proposed TS differ in two main ways compared to NZS 1170.5 [1]. Firstly, the proposed TS advocates for the use of spectral parameters that are defined for each location, site class and APoE to ensure the best representation of the NSHM2022 UHS when elastic demands are computed in functional form. This has been done to reflect observations that, in addition to site class, the spectral shape is affected by the intensity of ground shaking and earthquake magnitude, which vary from location to location. Secondly, for long periods  $(T > T_d)$ , the historical assumption of constant spectral displacement demand has been updated with an expression that gives slowly increasing spectral displacement demands. This has been done recognising that the earthquake magnitude affects the period at which spectral displacement demands plateau and the hazard at each site will be influenced by a range of possible earthquake magnitudes.

#### REFERENCES

- Standards New Zealand (2004). "NZS 1170.5—Part 5: Earthquake Actions—New Zealand". Standards New Zealand. <a href="https://www.standards.govt.nz/shop/nzs-1170-52004-excludes-amdt-1">https://www.standards.govt.nz/shop/nzs-1170-52004-excludes-amdt-1</a>
- 2 Lee RL, Cubrinovski M and Bradley BA (2025). "Site classification methodology for TS 1170.5 design spectra". Bulletin of the NZ Society for Earthquake Engineering, 58(1): 11-39. <a href="https://doi.org/10.5459/bnzsee.1686">https://doi.org/10.5459/bnzsee.1686</a>
- 3 Hulsey AM, Elwood KJ, Horspool N, Gerstenberger MC and Sullivan TJ (2025). "Assessing the life-safety risk for the proposed Technical Specification (TS) 1170.5". Bulletin of the New Zealand Society for Earthquake Engineering, 58(2): 119-133. https://doi.org/10.5459/bnzsee.1690
- 4 Housner GW (1941). "An Investigation of The Effects of Earthquakes on Buildings". PhD Dissertation. California Institute of Technology.

- 5 Sorrentino L (2007). "The early entrance of dynamics in earthquake engineering: Arturo Danusso's contribution". ISET Journal of Earthquake Technology, 44(1): 1–24.
- 6 Newmark NM (1959). "A method of computation for structural dynamics". *Journal of the Engineering Mechanics Division*, **85**(3): 67–94. https://doi.org/10.1061/JMCEA3.0000098
- 7 Chopra AK (2007). *Dynamics of Structures*. Pearson Education India.
- 8 Newmark NM (1970). "Current trends in the seismic analysis and design of high-rise structures". Selected Papers by Nathan M. Newmark: Civil Engineering Classics, 787–808.
- 9 Newmark NM, Blume JA and Kapur KK (1973). "Seismic design spectra for nuclear power plants". *Journal of the Power Division*, 99(2), 287–303. https://doi.org/10.1061/JPWEAM.0000753
- 10 Hayashi S, Tsuchida H and Kurata E (1972). "Average Response Spectra for Various Subsoil Conditions". McGraw Hill Book Company.
- 11 Kuribayashi E, Iwasaki T, Iida Y and Tuji K (1972). "Effects of seismic and subsoil conditions on earthquake response spectra". *International Conference on Micro*zonation, 499–512.
- 12 Seed HB, Ugas C and Lysmer J (1976). "Site-dependent spectra for earthquake-resistant design". *Bulletin of the Seismological Society of America*, **66**(1): 221–243.
- 13 American Society of Civil Engineers (2021). "ASCE 7-22: Minimum Design Loads and Associated Criteria for Buildings and Other Structures (7th Ed.)". American Society of Civil Engineers. https://doi.org/10.1061/9780784415788
- 14 McGuire RK (1974). "Seismic Structural Response Risk Analysis, Incorporating Peak Response Regressions on Earthquake Magnitude and Distance". Report R74-51, Structures Publication, 399. https://cir.nii.ac.jp/crid/1570291224295683712
- 15 Trifunac MD and Anderson JG (1978). "Preliminary Empirical Models for Scaling Pseudo Relative Velocity Spectra". Department of Civil Engineering, University of Southern California Berkeley.
- 16 Faccioli E, Paolucci R and Rey J (2004). "Displacement spectra for long periods". *Earthquake Spectra*, 20(2): 347– 376. https://doi.org/10.1193/1.1707022
- 17 Joyner WB and Boore DM (1982). "Estimation of Response-Spectral Values as Functions of Magnitude, Distance, And Site Conditions". US Geological Survey. https://pubs.usgs.gov/of/1982/0881/report.pdf
- 18 Joyner WB and Boore DM (1982). "Prediction of Earthquake Response Spectra". US Geological Survey Open-file Report. https://pubs.usgs.gov/of/1982/0977/report.pdf

- 19 Boore DM, Joyner WB and Fumal TE (1997). "Equations for estimating horizontal response spectra and peak acceleration from Western North American earthquakes: A summary of recent work". Seismological Research Letters, **68**(1): 128–153. <a href="https://doi.org/10.1785/gssrl.68.1.128">https://doi.org/10.1785/gssrl.68.1.128</a>
- 20 Somerville PG, Saikia C, Wald D and Graves R (1996). "Implications of the Northridge earthquake for strong ground motions from thrust faults". *Bulletin of the Seismological Society of America*, **86**(1B): S115–S125. https://doi.org/10.1785/BSSA08601BS115
- 21 Somerville PG and Graves RW (1996). "Strong ground motions of the Kobe, Japan earthquake of Jan. 17 1995 and development of a model of forward rupture directivity effects applicable in California". Western Regional Technical Seminar on Earthquake Engineering for Dams. Sacramento, California, 11-12.
- 22 Somerville PG, Smith NF, Graves RW and Abrahamson NA (1997). "Modification of empirical strong ground motion attenuation relations to include the amplitude and duration effects of rupture directivity". Seismological Research Letters, 68(1): 199–222. https://doi.org/10.1785/gssrl.68.1.199
- 23 Somerville PG, Krawinkler H and Alavi B (2000). "Development of Improved Ground Motion Representation and Design Procedures for Near-Fault Ground Motions". Final Report to CSMIP Data Utilization Program, 1097– 1601.
- 24 Weatherill G (2022). "Impact of Directivity on Probabilistic Seismic Hazard Calculations in New Zealand". Postdam: GFZ German Research Centre for Geosciences.
- 25 Bradley BA and Weatherill G (2025). "Consideration of near-fault effects in New Zealand seismic hazard analysis and design spectra". *Bulletin of the New Zealand Society for Earthquake Engineering*, **58**(2). https://doi.org/10.5459/bnzsee.1743
- 26 McVerry GH, Zhao JX, Abrahamson NA and Somerville PG (2006). "New Zealand acceleration response spectrum attenuation relations for crustal and subduction zone earthquakes". *Bulletin of the NZ Society for Earthquake Engineering*, **39**(1): 1–58. https://doi.org/10.5459/bnzsee.39.1.1-58
- 27 Abrahamson NA and Shedlock KM (1997). "Overview". Seismological Research Letters, 68: 9–23.
- 28 Boore DM (2010). "Orientation-independent, nongeometric-mean measures of seismic intensity from two horizontal components of motion". *Bulletin of the Seismological Society of America*, **100**(4): 1830–1835. https://doi.org/10.1785/0120090400

- 29 Boore DM (2006). "Orientation-independent measures of ground motion". Bulletin of the Seismological Society of America, 96(4A): 1502–1511. https://doi.org/10.1785/0120050209
- 30 Shahi SK and Baker JW (2014). "NGA-West2 models for ground motion directionality". *Earthquake Spectra*. 30(3): 1285-1300. https://doi.org/10.1193/040913EQS097M
- 31 Nievas CI and Sullivan TJ (2017). "Accounting for directionality as a function of structural typology in performance-based earthquake engineering design". Earthquake Engineering and Structural Dynamics, 46(5): 791–809. https://doi.org/10.1002/eqe.2831
- 32 Stewart JP, Abrahamson NA, Atkinson GM, Baker JW, Boore DM, Bozorgnia Y, Campbell KW, Comartin CD, Idriss IM, Lew M, Mehrain M, Moehle JP, Naeim F and Sabol TA (2011). "Representation of bidirectional ground motions for design spectra in building codes". *Earthquake Spectra*. 27(3): 927-937. https://doi.org/10.1193/1.3608001
- 33 CEN (2004). "Eurocode 8: Design of Structures for Earthquake Resistance—Part 1: General Rules, Seismic Actions and Rules for Buildings". (EN 1998-1: 2004). European Committee for Standardization.
- 34 American Society of Civil Engineers (2016). "ASCE 7-16: Minimum Design Loads and Associated Criteria for Buildings and Other Structures". American Society of Civil Engineers. https://doi.org/10.1061/9780784414248
- 35 Standards New Zealand (2004). "NZS 1170.5—Part 5: Earthquake Actions—New Zealand Commentary". Standards New Zealand. <a href="https://www.standards.govt.nz/shop/nzs-1170-5-supp-12004-excludes-amdt-1">https://www.standards.govt.nz/shop/nzs-1170-5-supp-12004-excludes-amdt-1</a>
- 36 Luco N, Ellingwood BR, Hamburger RO, Hooper JD, Kimball JK and Kircher CA (2007). "Risk-Targeted Versus Current Seismic Design Maps for the Conterminous United States".
- 37 American Society of Civil Engineers. (2021). "ASCET Hazard Tool" [Dataset]. <a href="https://asce7hazardtool.online/">https://asce7hazardtool.online/</a>
- 38 Subotić P, Muhadinović M, Sćepanović B and Lučić D (2024). "The future of seismic design of steel structures PR EN 1998-1-1 and PR EN 1998-1-2". *Journal of Applied Engineering Science*, 22(2): 303–309. https://doi.org/10.5937/jaes0-50730